Improvement proposal in the structural system of a15" R29 rigid mountain bike frame, with FEA and geometric optimization

Propuesta de mejora en el sistema estructural de un cuadro rígido de bicicleta de montaña de 15" R29, mediante FEA y optimización geométrica

Juan P. Guamán[1,*] ID, Hugo E. Crespo[1] ID,
César A. Paltán[2] ID, Jorge I. Fajardo[2] ID

Abstract

Currently, cycling has increased significantly, along with the implementation of mountain bikes (MTB) with rigid frames, which are employed both as a means of transportation and for competitions due to their affordable cost. Since these bikes serve various purposes, they present varying stresses on their frames, surpassing design requirements and leading to failures in the upper chainstays. This study analyzes this type of failure, for which information regarding the frame material, acting loads, and 3D modeling is collected. Subsequently, a failure homologation analysis is conducted, and a proposal for improvement is generated by applying geometric optimization, determining a thickness of 3.50 mm in the upper chainstays and guaranteeing the resistance of the bike frame under the study conditions; that is, a drop of 60 cm and a load of 74 kg. This modification ensures that the stress in the upper chainstays does not exceed the ultimate stress of the material of 890,94 MPa.

Keywords: rigid frame, MTB, chainstay, geometric optimization, ultimate stress, drop.

Resumen

En la actualidad la práctica del ciclismo ha tenido un incremento considerable, así como el uso de bicicletas de montaña (Mountain Bike, MTB, en inglés), de cuadro rígido, utilizadas como medio de transporte y para competencia, debido a su costo asequible. Este tipo de bicicletas, al ser utilizadas para varios propósitos, presentan esfuerzos variados en su cuadro, que conllevan a sobrepasar las exigencias de diseño, presentándose fallos en las vainas superiores. Este tipo de fallo es analizado en este estudio, motivo por el cual se levanta la información referente al material del cuadro, cargas actuantes y modelado 3D. Posterior se genera un análisis de homologación del fallo y se determina una propuesta de mejora aplicando optimización geométrica, donde se determina un espesor de 3,50 mm en las vainas superiores, garantizando la resistencia del cuadro de bicicleta bajo las condiciones de estudio; es decir, un drop de 60 cm y carga de 74 kg, con la cual se garantiza que el esfuerzo en las vainas superiores no sobrepase el esfuerzo último del material de 890,94 MPa.

Palabras clave: cuadro rígido, MTB, vainas superiores, optimización geométrica, esfuerzo último, drop.

[1,*]Mechanical Engineering, Universidad Politécnica Salesiana, Cuenca, Ecuador.
[2]New Materials and Transformation Processes Research Group GiMaT, Universidad Politécnica Salesiana, Cuenca, Ecuador. Corresponding author ✉: cpaltan@ups.edu.ec.

Guamán, et al. / Improvement proposal in the structural system of a15" R29 rigid mountain bike frame, with fea and geometric optimization

107

1. Introduction

The bicycle has become one of the most widely used alternative means of transportation, experiencing a significant increase in recent years [1, 2]. In addition to promoting health and being environmentally friendly, its accessibility makes it an affordable option for society [3, 4].

Considering the wide variety of bicycles, MTBs are the most commonly used due to their versatility and ability to ride on both roads and mountainous terrains [5]. These bicycles have front suspension, and their frame is rigid. Over time, bicycles have undergone a significant technological evolution, with a considerable reduction in weight and an increase in resistance, transitioning from the use of steel to composite materials reinforced with carbon fiber in most bicycle components and experiencing improvements in their transmission system [6].

Carbon Fiber Reinforced Polymer (CFRP) composites are used in manufacturing bicycle frames due to their advantages in lightweight, mechanical strength, and corrosion resistance [7]. It is worth noting that aluminium alloy inserts are incorporated in the interface areas with other bicycle components due to the type of connection [1]. The application of composite material in MTB bicycles is based on the arrangement or orientation of the fibers, using proposed filament braiding, which avoids excessive stiffness [8].

This vehicle comprises various components, one of the most important being the frame, as it holds the primary interfaces and is the point where stresses converge. Consequently, the frame is predisposed to failure due to the concentration of loads transmitted during operation [9].

Besides occurring at the joints and interfaces, the most common failures in rigid frames of MTB bicycles manifest in the upper and lower chainstays [10, 11]. This is due to overload caused by jumps or steep descents. Additionally, there are cases caused by falls, which are not considered failures in normal operation [12]. The analysis specifically focuses on the failure in the upper chainstays due to the physical configuration of a rigid frame.

It is essential to present a solution proposal since the failures are directly proportional to the increased use of rigid carbon fiber frame bicycles. This leads to greater customer dissatisfaction, resulting in a direct discredit of bicycle brands and, consequently, causing losses in sales [13].

By determining an improvement proposal through the geometric optimization of the upper chainstays [14], mechanical strength is ensured according to the design requirements of this type of bicycle, considering the desired input and output parameters [15], in line with the provisions of ISO 4210-6 2019 and its application [16].

In this article, the failure load and the configu-ration of the material used are determined. Then, a validation of the failure is carried out using engineering software. Subsequently, a solution proposal is presented through the geometric optimization of the upper chainstays [17].

2. Materials and Methods

2.1. Laminate configuration

An MTB bicycle manufactured with CFRP of dimensions 15" R29, was used, exhibiting a failure in the upper chainstays, as illustrated in Figure 1.

Figure 1. Failure in the upper chainstays

In this case, for the application of the bicycle frame, a quasi-isotropic laminate is used, with layers oriented in [0°, 45°, –45°, 90°]. This quasi-isotropic carbon fiber laminate offers several significant advantages, such as good performance in terms of strength and stiffness in multiple planes. It also provides greater durability due to better load distribution, increasing the material's resistance to fatigue. This is especially valuable in applications where the laminate is subject to variable or cyclic loads over time. Another factor is the reduction in sensitivity to cracks, as it is less prone to crack propagation or localized damage, in addition to better vibration absorption. These characteristics result from its structure and uniform distribution of carbon fibers in multiple directions [18].

Carbon fiber sheets are composed of filaments containing a percentage between 80 and 95% carbon, with a diameter usually around 8 µm. A resin or polymeric matrix is used to position and bond these filaments and protect them from external agents [19, 20].

Figure 2 illustrates the orientation system of carbon fibers subjected to tensile and compressive stress, considering fiber orientation [19, 21].
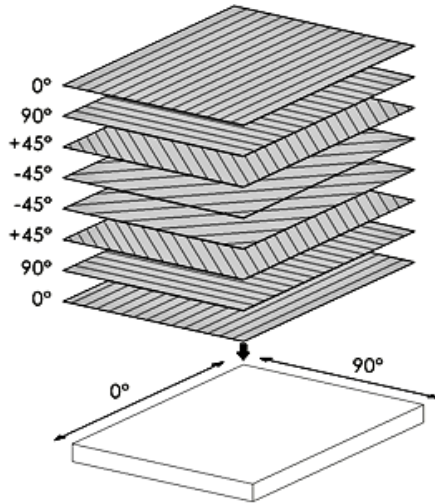
Figure 2. Quasi-isotropic laminate [20]

Table 1 shows the epoxy/carbon composite material constants.

Table 1. Composite material constants

Exy	Eyz	Exz
Young's Modulus (GPa)		
123.3	7.78	7.78
Vxy	**Vyz**	**Vxz**
Poisson's Ration		
0.27	0.42	0.27
Gxy	**Gyz**	**Gxz**
Shear Modulus (GPa)		
5	3.8	5

2.2. Methods of analysis

To analyze carbon fiber bicycle frames, a quasi-isotropic laminate is used with the following fiber orientation and arrangement angles: 0º / 90º / +45°/ –45°/ –45°/ +45/ 90º / 0º, which are loaded into the program configuration as layers before conducting simulations.

Furthermore, in the material analysis, orthotropic symmetry is taken as a reference, and the material constitutive equation in equation (1) is considered for a Cartesian system with three mutually perpendicular directions, where the stresses (σ) are equal to the product of the stiffness matrix (C) and the deformations (ε) [19].

$$\begin{Bmatrix} \sigma1 \\ \sigma2 \\ \sigma3 \\ \tau23 \\ \tau31 \\ \tau12 \end{Bmatrix} = \begin{bmatrix} C_{11} & C_{12} & C_{13} & 0 & 0 & 0 \\ C_{21} & C_{22} & C_{23} & 0 & 0 & 0 \\ C_{31} & C_{32} & C_{33} & 0 & 0 & 0 \\ 0 & 0 & 0 & C_{44} & 0 & 0 \\ 0 & 0 & 0 & 0 & C_{55} & 0 \\ 0 & 0 & 0 & 0 & 0 & C_{66} \end{bmatrix} \begin{Bmatrix} \varepsilon_1 \\ \varepsilon_2 \\ \varepsilon_3 \\ \gamma_{23} \\ \gamma_{31} \\ \gamma_{12} \end{Bmatrix} \quad (1)$$

Where:

- $\sigma_{1,2,3}$ = Stresses in the x, y, and z directions

- $\tau_{1,2,3}$ = Shear in the x, y, and z directions

- $[C]$ = Stiffness matrix

- $\varepsilon_{1,2,3}$ = Deformations in x, y, and z

- $\gamma_{1,2,3}$ = Angular deformation in x, y, and z

2.3. Finite element model used

The finite element model used in this study is the Von Mises model, which determines the deformations generated on the chainstays. The analysis is static, as the loads influencing the bicycle frame and the correlation of dynamic loads are known. Tetrahedral elements are employed for meshing due to the complexity of the model, and the element order number is quadratic, contributing to convergence [9]. Regarding the type of laminate bonding in practical cases, Bonded is used due to its process, and for the simulation, a laminate was loaded as a Layered Section, allowing the specification of the thickness and angles of each layer.

2.4. Failure criterion

The failure criterion is based on the maximum normal stress since the material is brittle; in this case, the bicycle frame, made of carbon fiber, undergoes minimal deformation before breaking. For validation, failure occurs when one of the stress components in the three orthogonal directions is greater than or equal to the material's stress limit in the corresponding direction, as indicated in equation (2).

$$\sigma_{max} = max(|\sigma_1|, |\sigma_2|, |\sigma_3|) \geq \sigma_u \quad (2)$$

Where:

- σ_{max} = Maximum stress

- $\sigma_1, \sigma_2, \sigma_3$ = Stress in x and z

- σ_u = Ultimate stress

2.5. Geometric optimization

The objective of the geometric optimization in this case study is to maximize the thickness of the upper chainstays to increase resistance and thereby withstand the stresses generated by the load acting on the bicycle frame. It is crucial to identify the input and output parameters or conditions necessary to obtain the appropriate values according to the established requirements.

The input condition is:

- **P4**: Thickness

Guamán, et al. / Improvement proposal in the structural system of a15" R29 rigid mountain bike frame, with fea and geometric optimization

109

The output conditions are:

- **P2**: Restriction of the ultimate material stress (890 MPa) and thickness range from 1 to 5 mm

- **P3**: Maximize the volume

2.6. Characterizations

2.6.1. Microscopy analysis

To determine the thickness of the laminate, a sample was taken from the area near the break in the upper chainstay, which was prepared following the metallographic procedure [22]. The micrograph of the analyzed region provided the image shown in Figure 3.

Figure 3. Microscopy 5x (a) and 20x (b)

With the microscopic analysis at 20x, it is determined that the thickness of the laminate is 125 μm [23], indicating that, according to the raised thickness of 1 mm in the upper chainstay, there are 8 sheets, as mentioned in [24–26].

2.6.2. Data sensor

The bicycle user, using a Mobvoi Ticwatch E3 sports bracelet equipped with GPS, gyroscope, accelerometer, and heart rate monitor sensors, recorded data such as bicycle speed, terrain slope, and jump height.

2.6.3. Thickness analysis

To determine the thickness of the laminate in the upper chainstays of the bicycle frame, An Olympus BX51M metallographic microscope with a DP72 digital camera was used, along with the OLYMPUS Stream Essential® software, which allows capturing images at magnifications of 5x and 20x.

### 2.7. Bicycle frame geometry

The geometry of the bicycle frame is modeled as a 1:1 scale surface, allowing the loading of the laminates with their respective orientation of quasi-isotropic fibers. Figure 4 displays the model of the rigid bicycle frame.

Figure 4. 3D frame geometry

2.8. Meshing

A meshing of the geometry surface is performed, using the Capture Proximity and Curvature mesh enhancement method. 81786 nodes and 82487 elements were obtained (Figure 5).
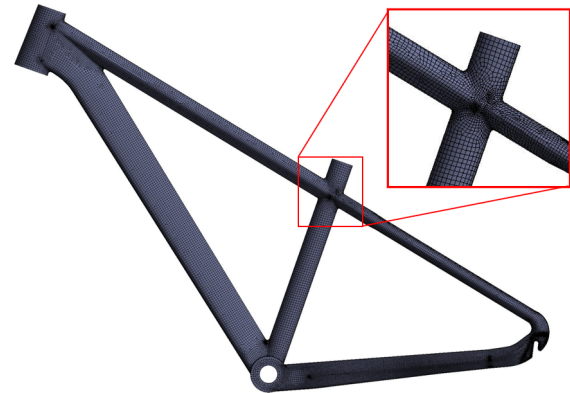
Figure 5. Bicycle frame meshing

In the mesh quality verification, average values of Orthogonal Quality: 0.97 and Skewness: 0.14 are obtained. These results indicate a high mesh quality [26], ensuring an appropriate approximation of the simulation values.

2.9. Determination of failure factors

The data collected from the sports bracelet used by the cyclist on the day of the event include a speed of 35 km/h, a route slope of -2°, and a drop or jump of 0.60 m in height. Additionally, it is known that the mass of the cyclist is 74 kg, which acted on the bicycle saddle.

2.10. Determination of the ultimate tensile stress of the laminate

With the information on the layers thickness with its respective orientation and the acting load, the ultimate tensile stress of the bicycle frame laminate can be determined.

To simulate the tensile test, a specimen model measuring 25 mm wide x 150 mm long and 2.50 mm thick with eight layers of laminate with quasi-isotropic configuration is generated. The boundary conditions include a fixed end and a displaced end, where a displacement of 4 mm is applied in the longitudinal direction of the specimen, following the standards established in ASTM D3090 [27]. The analysis was conducted using Explicit Dynamics, obtaining the maximum equivalent Von Mises stress (514,87 MPa), as shown in Figure 6.
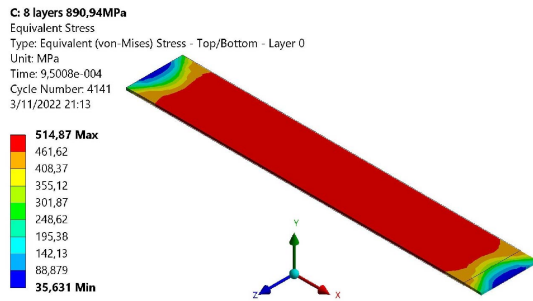

Figure 6. Tensile test specimen simulation

After performing the simulation of the tensile test specimen, a maximum tensile stress of 890,94 MPa is obtained.

2.11. Numerical simulation of vertical load

The vertical load test method of UNE ISO 4210-6 [16] describes boundary conditions that apply to this analysis, thus complementing the information described in the failure mode determination section (Figure 7).
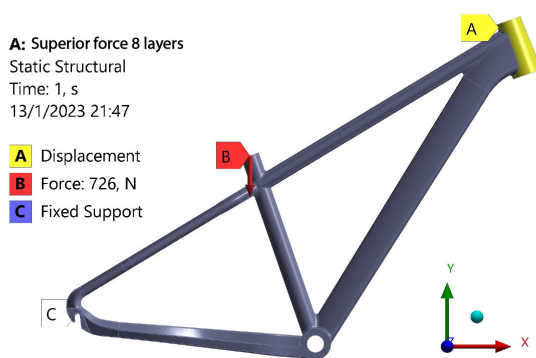

Figure 7. Initial and boundary conditions

Additionally, the standard specifies that the tests to be applied are dynamic; however, the analysis of this bicycle frame will be carried out statically, applying values relative to dynamic loads to achieve the same effect [28, 29].

Equation (3) is used to calculate the dynamic coefficient. Then, the dynamic force is calculated using equation (4).

$$K_d = 1 + \sqrt{1 + \frac{2 * H}{\delta_{est}}} = 46,119 \qquad (3)$$

Where:

- H= Bicycle drop height (mm)

- δ_{est} = Static displacement of the point of application of the static force (mm)

To determine the static displacement at the load application point, a preliminary simulation is conducted, applying a load of 74 kg, and resulting in a displacement of 0.52 mm (Figure 8).
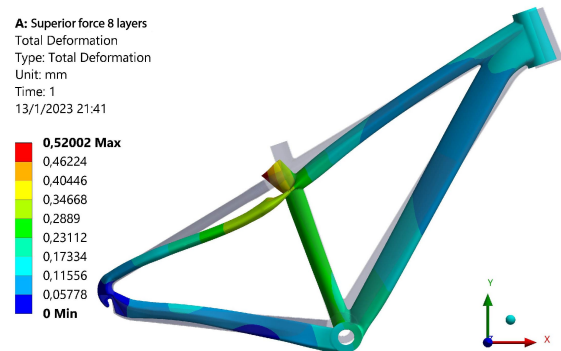

Figure 8. Maximum displacement with a static load of 74 kg

Thus, the dynamic load is determined.

$$P_d = P_e * K_d = 3412,80 \ kg \qquad (4)$$

Where:

- P_e = Static force

The Pd value is the new load applied to carry out a second simulation, considering the impact of the initial load of 74 kg, with a drop height of 0.60 m.

3. Results and Discussion

3.1. Rupture of the upper chainstays

To determine the equivalent Von Mises stress acting on the upper chainstays to homologate the failure mode, a load of –3412,80 kg (Pd) is applied to the "Y" axis of the seat tube, representing the cyclist's load. After post-processing, values exceeding the ultimate stress of 890.94 MPa (determined with the specimen) are obtained, as shown in Figure 9. The failure mechanism occurs due to impact and repetitive stress; cracks that are not detected in time and that can propagate and weaken the bicycle structure may appear. In this study, no delamination is observed because the carbon fiber layers do not separate or detach, as demonstrated in the bicycle frame inspection using microscopy. Impact damage weakens the structure and reduces its strength. A forceful impact against a hard object or a significant

Guamán, et al. / Improvement proposal in the structural system of a15" R29 rigid mountain bike frame, with fea and geometric optimization

111

fall can cause internal damage not visible to the naked eye. Additionally, the overload from the jump exceeded the design limits.
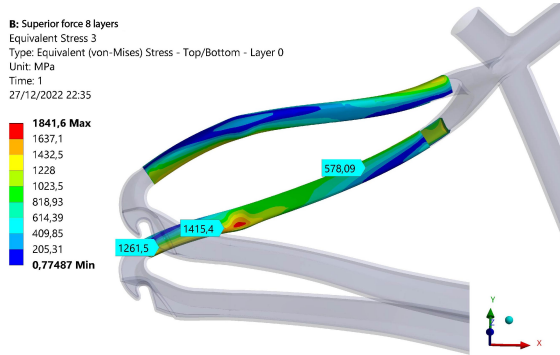

Figure 9. Stresses generated in the upper chainstays

3.2. Analysis through geometric optimization

3.2.1. Optimization of the bicycle frame thickness

Considering the ultimate stress of the laminated material specimen of 890.94 MPa, the stress obtained in the rupture zone of the upper chainstays of 1415.40 MPa, and maximum stress of 1841.60 MPa displaced towards the rupture zone, located in the subsequent left zone, as shown in Figure 9, an optimization is performed to prevent this stress from affecting the upper chainstays.

After the first iteration, three candidate points are obtained as a solution, as shown in Table 2. These points represent the three possible thickness options for the bicycle frame laminate. Candidate point 1 corresponds to a thickness of 5 mm, representing a 400% increase in thickness; candidate point 2 corresponds to a thickness of 4.60 mm, representing a 360% increase; and candidate point 3 corresponds to a thickness of 4.16 mm, representing a 316% increase. Point 3 shows the smallest increase among all; therefore, it can be considered for the simulation with the new thickness.

Table 2. Geometric optimization results. First optimization.

Name	P4-SYS\ Surface Thickness (mm)	P2 – Equivalent Stress 3 Máximum (MPa)		P3 - SYS \Surface Volume (mm^3)	
		Parameter value	Variation in relation to the reference	Parameter value	Variation in relation to the reference
Candidate point 1	5	2167,6	0,45 %	1,93E+0,6	20,09 %
Candidate point 2	4,6	2164,1	0,29 %	1,78E+0,6	10,48 %
Candidate point 3	**4,16**	**2157,8**	**0,00 %**	**1,61E+0,6**	**0,00 %**

By conducting another simulation with the new thickness of 4.16 mm throughout the bicycle frame, a stress of 478.68 MPa is obtained in the failure zone,

and a maximum stress of 665 MPa in the subsequent left zone. See Figure 10a.

3.2.2. Optimization of the upper chainstays thickness

The second iteration focuses exclusively on the thickness of the upper chainstays, using the results from the first run and referencing the maximum stress of 665 MPa. As a result, three candidate points with new thickness values are obtained, as shown in Table 3. The objective of this second iteration is to reduce the thickness of the upper chainstays compared to the thickness found for the rest of the frame. Candidate point 1 was discarded because it has a value of 4.16 mm. From the remaining candidate points, the one with the least thickness was selected, which was point 3 with a value of 3.50 mm.

A new simulation was conducted with the new thickness value of 3.50 mm in the upper chainstays of the bicycle frame, resulting in a stress of 604.60 MPa in the failure zone and a maximum stress of 714.94 MPa in the subsequent left zone. See Figure 10b.
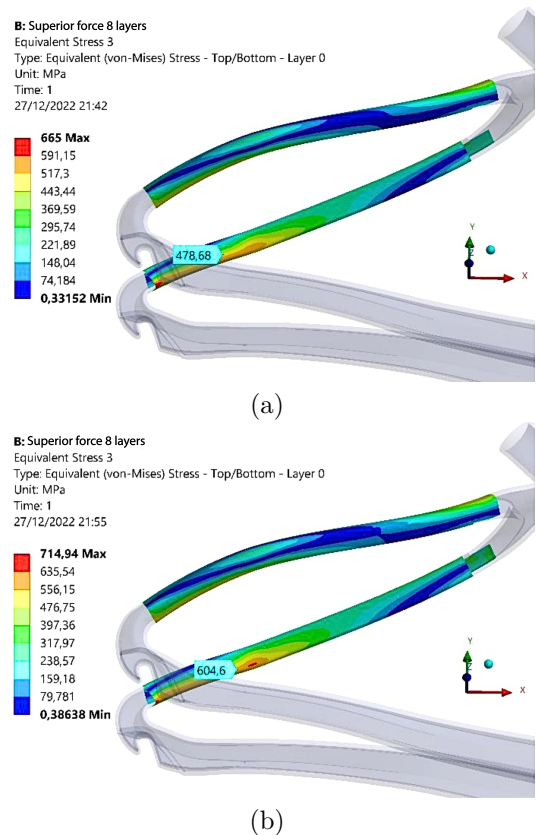

(a)

(b)

Figure 10. Stresses generated in the upper chainstays in the first iteration (a). Stresses generated in the upper chainstays in the second iteration (b).

Table 3. Geometric optimization results. Second optimization

Name	P4-SYS\ Surface Thickness (mm)	P2 – Equivalent Stress 3 Máximum (MPa)		P3 - SYS \Surface Volume (mm^3)	
		Parameter value	Variation in relation to the reference	Parameter value	Variation in relation to the reference
Candidate point 1	4,16	664,97	0,00 %	1,61E+0,6	18,89 %
Candidate point 2	3,84	664,97	0,00 %	1,491E+0,6	9,85 %
Candidate point 3	**3,5**	**664,97**	**0,00 %**	**1,358E+0,6**	**0,00 %**

3.2.3. Final proposal

Table 4 shows the final results of the optimizations:

Table 4. Final results of the optimizations

Parameters	Initial state	Optimized state	Variation
Stress in the upper chainstays	1766 MPa	619,54 MPa	–64,92 %
Material thickness	1 mm	3,50 mm	250,20 %

4. Conclusions

Currently, rigid-frame mountain bikes are widely used, both as a means of transportation and in competitions. Often, users tend to overuse them due to their versatility and affordability, disregarding their application limits and employing them in situations for which they were not originally designed.

The study allowed identifying the mechanisms to determine failures in carbon fiber bicycle frames, analyzing the failure mode of the upper chainstays after a 60 cm drop, based on the UNE ISO 4210-6 standard and collecting user data. Validation was carried out through Finite Element Analysis (FEA).

Microscopy analysis allowed determining the thickness and number of layers, as well as the total thickness of the laminate.

It is valid to note the determination of the number of layers (8 layers) and, considering previous studies on the standard laminate of commercial carbon fiber bicycle frames (quasi-isotropic), a tensile analysis is performed. In this analysis, ultimate load values are obtained, and a stress-deformation curve is generated for a brittle material.

To perform the analysis in the numerical simulation program, the Layered Section laminate is loaded, configuring the number of layers and their orientation. This allows for establishing a similarity with the

"bonded" laminate used in the manufacture of carbon fiber bicycle frames.

The failure of the bicycle frame components, specifically in the upper chainstays, occurs when the generated stresses exceed the ultimate stress of the composite material, which is 890.94 MPa, according to the simulation conducted on the laminate specimen.

The geometric optimization is based on the proposal of new thickness values for the laminated material and not on the variation of its geometry. Furthermore, the improvement proposal guarantees the stresses generated by the cyclist's load, considering a weight of 74 kg and a drop of 60 cm.

Optimization proposes a thickness of 3.50 mm for the upper chainstays. Additionally, a thickness of 4.16 mm is proposed for the rear wheel attachment area, as it directly impacts the upper chainstays.

The rupture of the system under study is due to the inherent fragility of the material. The observed deformation is characteristic of a fragile system, and the rupture occurs because of the fragility of the carbon fiber. By proposing a thickness of 3.5 mm through optimization, it is possible to prevent breakages caused by impacts when the bicycle falls to the ground during the analyzed jumps. This result is attributed to the increased area, thus avoiding exceeding the stress limit of the composite material.

References

[1] S. M. Martín Mozas, *Desarrollo de guía metodológica y ejemplo de análisis estático y a fatiga de cuadro de bicicleta.* E. T. S. I. Industriales. Universidad Politécnica de Madrid, 2021. [Online]. Available: https://bit.ly/48wefnU

[2] J. Freire, *El sector de la bicicleta en cifras 2020.* 30 Días en Bici, 2020. [Online]. Available: https://bit.ly/3ruvJAf

[3] W. J. Jara Lupercio and M. A. Dunia Pauta, *Beneficios sobre la salud derivados del uso de la bicicleta, frente a la contaminación ambiental y la pandemia SARS CoV-2. Revisión bibliográfica.* Carrera de Cultura Física. Universidad de Cuenca, 2021. [Online]. Available: https://bit.ly/48rqrpO

[4] J. Sanín Eastman, "El uso de la bicicleta como promotor de la movilidad sostenible: acciones y efectos en la movilidad cotidiana, el mejoramiento de la calidad del aire y el transporte público de las ciudades," *Revista Kavilando*, vol. 12, no. 1, pp. 118–126, jun. 2020. [Online]. Available: https://bit.ly/45a030G

[5] P. Cañizares Gómez de Terreros, *Prediseño y análisis numérico de un prototipo de cuadro de*

Guamán, et al. / Improvement proposal in the structural system of a15" R29 rigid mountain bike frame, with fea and geometric optimization

113

bicicleta en CFRP. Universidad de Sevilla, 2016. [Online]. Available: https://bit.ly/3Pt8DSx

[6] P. Navarro, J. Rui-Wamba, A. Campos, O. Antisench, C. Bañuelos, and M. Jordi, J. Rui-Wamba, *Ingeniería de la Bicicleta.* Fundación Esteyco, 2009. [Online]. Available: https://bit.ly/466mHIC

[7] P. Bajpai, *Carbon Fiber.* Second edition. Cambridge, Elsevier, 2020. [Online]. Available: https://bit.ly/453CAOU

[8] A. Paz Carvajal, L. M. Ríos Gamboa, G. F. Casanova García, A. Leyton, and J. J. García Álvarez, "Fabricación y caracterización mecánica de un laminado de fibra de carbono en matriz de resina epoxi," *Scientia et Technica*, vol. 22, no. 3, pp. 262–267, 2017. [Online]. Available: https://bit.ly/465xoev

[9] K. Khutal, G. Kathiresan, K. Ashok, B. Simhachalam, and D. Davidson Jebaseelan, "Design validation methodology for bicycle frames using finite element analysis," *Materials Today: Proceedings*, vol. 22, pp. 1861–1869, 2020, 2nd International Conference on Materials Manufacturing and Modelling, ICMMM – 2019, VIT University, Vellore, 29th - 31st March 2019. [Online]. Available: https://doi.org/10.1016/j.matpr.2020.03.085

[10] Aszahara. (2010) Rotura tirante carbono Orbea Oiz, garantía. Foro MTB. Foro MTB. [Online]. Available: https://bit.ly/3ZvqFbf

[11] NazcaCarbono. (2020) Caso de éxito: Reparación de una vaina totalmente seccionada. Nazca Carbono. [Online]. Available: https://bit.ly/3rsOqnP

[12] UvesBikes. (2023) Reparar cuadro de bicicleta. Uves Bikes. Uves Bikes. [Online]. Available: https://bit.ly/3rAvt2u

[13] C. Carlson Morales and A. L. Villarreal-Gómez, "Análisis de las 5 fuerzas de Porter aplicado a una refaccionaria de bicicletas y motocicletas," *Boletín Científico de las Ciencias Económico Administrativas del ICEA*, vol. 8, no. 16, pp. 44–47, jun. 2020. [Online]. Available: https://doi.org/10.29057/icea.v8i16.5832

[14] M. A. Guzmán and A. Delgado, "Optimising a shaft's geometry by applying genetic algorithms," *Ingeniería e Investigación*, vol. 25, no. 2, pp. 15–23, 2005. [Online]. Available: https://doi.org/10.15446/ing.investig.v25n2.14631

[15] U. Khalid, O. M. A. Mustafa, M. A. Naeem, M. Y. M. Alkhateeb, and B. M. A. E. Awad, "Direct optimization of an automotive sheet metal part using ANSYS," *International Journal of Engineering and Management Sciences*, vol. 5, no. 3, pp. 134–142, 2020. [Online]. Available: https://doi.org/10.21791/IJEMS.2020.3.14

[16] ISO, *ISO 4210-6:2023 Cycles – Safety requirements for bicycles – Part 6: Frame and fork test methods.* Internacional Organization for Standardization, 2023. [Online]. Available: https://bit.ly/3LCmg0m

[17] L. Parras, "Métodos alternativos de optimización de la geometría de estructuras articuladas," *Informes de la Construcción*, vol. 35, no. 351–352, pp. 77–82, 1983. [Online]. Available: https://bit.ly/3Zy91DG

[18] J. Fajardo, M. Villa, J. Pozo, and D. Urgilés, "Characterization of the tensile properties of an epoxy-carbon laminated composite used in the development of a single-seater Formula SAE type," *Enfoque UTE*, vol. 10, no. 3, pp. 1–12, 2019. [Online]. Available: https://doi.org/10.29019/enfoque.v10n3.381

[19] A. F. Rivas Bolívar, *Análisis estructural de un marco rígido de bicicleta de montaña mediante el modelamiento de elemento finitos en el software ANSYS.* Facultad de Ingeniería. Universidad de los Andes, 2019. [Online]. Available: https://bit.ly/48wxeP9

[20] L. A. Vargas Martínez and J. M. Martínez Benavides, *Estudio de propiedades mecánicas en láminas de fibra de carbono fabricadas mediante el proceso de laminación para elementos aeronáuticos.* Universidad Tecnológica de Pereira, 2019. [Online]. Available: https://bit.ly/3PwqDvd

[21] R. M. Jones, *Mechanics of composite materials.* Taylor and Francis, 1999. [Online]. Available: https://bit.ly/3ro9DiT

[22] Facultad de Ingeniería, *Metalografía Protocolo. Curso de Materiales.* Escuela Colombiana de Ingeniería Julio Garavito, Colombia, 2011. [Online]. Available: https://bit.ly/3t5aw0i

[23] S. K. García Castillo, *Análisis de laminados de materiales compuestos con precarga en su plano y sometidos a impacto.* Departamento de Mecánica de Medios Continuos y Teoría de Estructuras. Universidad Carlos III de Madrid, 2007. [Online]. Available: https://bit.ly/46ooad5

[24] E. Monsalvo Barrera and J. Cortés Rico, *Propuesta de diseño de una masa soporte en fibra de carbono para un vehículo mini-baja.* Facultad de Ingeniería. Universidad Nacional Autónoma de México, 2012. [Online]. Available: https://bit.ly/3ZsUl93

[25] A. Solana Rodríguez, *Cuadro de bicicleta en material compuesto.* Departamento de Ingeniería Mecánica, Energética y de Materiales. Universidad Pública de Navarra, 2014. [Online]. Available: https://bit.ly/3ZzFkSP

[26] ANSYS, *Mesh Quality.* ANSYS Workbench, 2023. [Online]. Available: https://bit.ly/3RBFMyc

[27] ASTM, *ASTM D3039/D3039M-08 Standard Test Method for Tensile Properties of Polymer Matrix Composite Materials.* ASTM International, 2014. [Online]. Available: https://bit.ly/3PzA6SJ

[28] Y. Lugo Pérez, *Modelación de un cuadro de bicicleta "Minerva" para la utilización de un nuevo material aplicando el MEF.* Ingeniería Mecánica, 2006. [Online]. Available: https://bit.ly/3rtgUxQ

[29] D. Vdovin, Y. Levenkov, and V. Chichekin, "Light frame design for quad bike using topology optimization," *IOP Conference Series: Materials Science and Engineering*, vol. 589, no. 1, p. 012026, 2019. [Online]. Available: https://dx.doi.org/10.1088/1757-899X/589/1/012026